

# Static and Dynamic Solvation at the Air/Water Interface<sup>†</sup>

David Zimdars<sup>‡</sup> and Kenneth B. Eisenthal\*

Department of Chemistry, Columbia University, New York, New York 10027

Received: June 5, 2000

The electronic excited-state solvation dynamics of coumarin 314 (C314) adsorbed at the air/water interface was investigated by femtosecond time-resolved second-harmonic generation (TRSHG). The second-harmonic spectrum of C314 at the air/water interface was determined using a tunable optical parametric generator, giving a spectral peak at  $419 \pm 3$  nm. The solvatochromic shift is in good agreement with the recently proposed interfacial polarity scale, which predicts that the empirical polarity parameter of the interface is the arithmetic mean of the two bulk phases. The time-resolved second-harmonic response to the excited-state solvation was measured at two fundamental wavelengths (840 and 900 nm) and with two pump polarizations (S and P). The results indicate that the static spectral peaks of the S- and P-pumped distributions are offset  $\sim 5$  nm, while the dynamic interfacial solvation proceeds with two time constants,  $\tau_1 = \sim 200$  fs and  $\tau_2 = 1.2$  ps, which are independent of C314 interfacial orientation. The slight blue shift of the C314 molecules closer to the normal incidence indicates that the electronic spectra of species at the air/water interface is inhomogeneously broadened by orientation, an effect which had not been observed previously. This can be described by a static solvation that depends on the orientation of the molecule's dipole moment at the interface. The dynamic solvation times are consistent with bulk experiment, as well as theory, which indicates that the air/water relaxation times, which are controlled by water/water interactions, should not be different from the bulk values.

## 1. Introduction

The physical and chemical properties of interfaces are of great importance to fundamental science, medicine, and technology.<sup>1–4</sup> Intrinsic to the interface is the asymmetrical environment experienced by the chemical species at the interface,<sup>5,6</sup> whether they are in the form of a solid or a molecular species, as in a gas or liquid, or are interface charges made up of electrons or ions. Because of this asymmetry, the interface provides a unique solvent environment with properties that differ from either bulk phase.

The solvent plays a fundamental role in chemical and physical processes in bulk solution. The ground and excited-state energies of a solute are modified by the organization of the solvent about the solute molecules. More generally, the potential surfaces, intersections, and barriers that separate different molecular states and structures can all be modified by the solvent. Solvation is a complicated process that depends on both nonspecific interactions arising from electrostatic and polarization forces as well as specific forces such as hydrogen bonding. The effects of the solvent are both static and dynamic. The position, shape, and intensity of static fluorescence and absorbance bands are determined by the solvent medium that are often described in terms of the solvent's polarity. Polarity is an empirical parameter, for which several scales exist, that list a solvent according to its solvating strength.

Many molecules exhibit solvatochromism, i.e., the position of the molecule's electronic UV/vis absorbance band shifts with

the polarity of the solvent. The direction and magnitude of a solvatochromic spectral shift depends on the solvent/solute interactions. Generally, a red (bathochromic or positive) shift with increasing solvent polarity occurs when the excited state is more dipolar than the ground state ( $\mu_g < \mu_e$ ,  $\mu_g$  and  $\mu_e$  are the ground and excited-state permanent dipole moments). The electronic transition energy decreases because the more dipolar excited state is stabilized by more polar solvents. Likewise, a blue (hypsochromic or negative) shift with increasing solvent polarity occurs when the excited state is less dipolar than the ground state ( $\mu_e < \mu_g$ ). The electronic transition energy increases because the less dipolar excited state is less stabilized than the ground state for more polar solvents.

Solvation has dynamic properties as well, as for example when a solvent reacts to an instantaneous photophysical change in the solute's charge distribution. This is the process responsible for the ultrafast time dependent shift of the fluorescence spectral peak (Stoke's shift). If the ground and excited states of a solute have sufficiently different permanent dipole moments ( $\mu_g \neq \mu_e$ ), the polar solvent reorganizes about the solute upon photoexcitation. Initially, the solvent shell is organized in a way to minimize the free energy of the ground state with dipole moment  $\mu_g$ . Immediately upon excitation the solute has the dipole moment  $\mu_e$ . However, the solvent shell is still in a configuration best suited for the ground state. The solvent shell rapidly reorganizes in reaction to the changed dipole moment of the excited state solute, decreasing the energy between the ground and excited states. This solute reorganization occurs on a time scale characteristic of the solvent. A schematic diagram of the electronic excited state solvation process has been presented previously (see Figure 2 in ref 7).

Recently, we have presented reports on the static solvatochromism of the solutes *N*, *N'*-diethyl-*p*-nitroaniline (DEPNA)

<sup>†</sup> Part of the special issue "John T. Yates Festschrift".

\* To whom correspondence should be addressed. Fax: (212) 839-1289. E-mail: eisenth@chem.columbia.edu.

<sup>‡</sup> Current address: Picometrix, Inc., 2901 Hubbard Road, Ann Arbor, MI 48105; Email: dzimdars@picometrix.com.

**TABLE 1: Correlation of Spectral Peak to  $E_T(30)$  Polarity Parameter<sup>a</sup>**

solvent	$E_T(30)$	absorbance (nm)	fluorescence (nm)
water	63.1	448	488
methanol	55.5	438	483
1-butanol	50.2	436	479
2-methyl-2-propanol	43.9	433	472
chlorobenzene	37.5	432	465
<i>n</i> -hexane	30.9	416	429
air/water	31.1	417 (419)	430

<sup>a</sup> The absorbance and fluorescence maxima of coumarin 314 are given with the  $E_T(30)$  polarity parameter in a series of solvents. The predicted air/water interface polarity parameter and predicted maxima for coumarin 314 are shown at the bottom of the table. The measured value for the air/water SH spectral peak is shown in parentheses.

and the betaine dye 4-(2,4,6-triphenylpyridinium)-2,6-diphenylphenoxide ( $E_T(30)$ ), at air/liquid and liquid/liquid interfaces as measured by surface specific second harmonic (SH) spectroscopy. The bulk liquid solvatochromism of these dyes is used to define the  $\pi^*$  and  $E_T(30)$  bulk polarity scales, respectively. For several interface systems studied, it was found that the interface polarity is equal to the arithmetic average of the polarity of the adjoining bulk phases. It was proposed that this result is general and can be used to assign and predict empirical polarity values to liquid interfaces.

We have also recently studied the electronic excited-state solvation dynamics of coumarin 314 (C314) at the air/water interface by time-resolved second-harmonic generation (TR-SHG).<sup>7,8</sup> The ground-state C314 has a large permanent dipole moment of 8.2 D.<sup>9</sup> Upon excitation, the dipole moment of C314 increases to about 12 D.<sup>10</sup> This large difference in permanent dipole moment yields bathochromic shifts with solvent polarity and makes C314 a good probe of electronic excited-state solvation dynamics. Our preliminary study demonstrated that solvation can be studied by TRSHG, and we found that the electronic excited-state solvation time at the air/water interface was close to the results in bulk water. The dynamic solvation time at the air/water interface was found to be in qualitative agreement with simple dielectric continuum models as well as the predictions of molecular dynamics.

The surface specificity of SH spectroscopy offers a great advantage over other methods sensitive to static and dynamic solvation which might be applied to the interface. The second-harmonic (SH) signal is generated only by the chosen interfacial adsorbate (see refs 1 and 2 for reviews of SH spectroscopy). There is no interference from the bulk solute, since SH is an electric dipole forbidden by symmetry in isotropic bulk media.<sup>1,2</sup> Only those probe molecules present at the interface where inversion symmetry is broken can contribute to the SH signal.

In the present study, both the static and dynamic solvation of coumarin 314 (C314) at the air/water interface were investigated by surface second-harmonic generation. The second-harmonic spectra of C314 at the air/water interface was determined using a tunable optical parametric generator. The solvatochromism of C314 in bulk liquids was shown to be well-correlated to the  $E_T(30)$  polarity scale (Table 1), allowing the C314 electronic absorbance peak to be predicted from the previously calibrated  $E_T(30)$  value of the air/water interface. The transition energy of the measured SH spectrum of C314 at the air/water interface (419 nm) was found to agree with the predicted value of 417 nm, further indicating that the polarity of a liquid interface can be obtained from the average of the bulk polarities. At first glance, it might be assumed that this simple result implies that the absorbance spectra of an interfacial adsorbate is homogeneously broadened as it is in a bulk liquid.

However, it will be shown that the electronic absorbance spectra of C314 at the air/water interface is in fact *inhomogeneously* broadened by its asymmetric environment and that it is only the ensemble average transition energy which corresponds to the "average" interfacial polarity.

The ensemble of adsorbates at the air/water interface is substantially different from an ensemble of solute in bulk water. For example, inside the water bulk, dissolved molecules would point, rotate, and diffuse in all directions. In comparison, the motions of an adsorbate molecule at the air/water interface are restricted by an asymmetric surface potential energy. One end of a molecule may prefer to stick down into the water, and the other end may prefer to stick up into the air. Because of these differences between the in-plane and out-of-plane potentials, the asymmetric surface environment results in an anisotropic distribution of solute. The in-plane,  $\varphi$ , angular distribution is isotropic at equilibrium because the in-plane intermolecular forces are isotropic. However, the asymmetry in forces normal to the interface, e.g. air above and water below the interface, results in adsorbate orientation in the out-of-plane angle  $\theta$ . The orientational distribution can be depicted schematically (see Figure 1B in ref 11) as lying between two cones, i.e., principally oriented between the  $\theta$  values of the two cones. For C314 at the air/water interface, the out-of-plane distribution in the ground state was measured to be peaked near 80° by the null angle technique.<sup>1,11</sup>

This potential asymmetry can change the dynamics of the adsorbate. Recently, we have used TRSHG to study the rotational motions of C314 at the air/water interface, which is the same molecular system as the solvation studies in this report. We have shown that the rotational motions within the plane of the interface are no longer equivalent to rotational motions out of the plane of the interface. The out-of-plane rotation time (350 ps) was found to differ substantially from the in-plane rotation time (600 ps).

Likewise, if the asymmetry provides orientationally dependent solvation environments, the electronic absorbance spectra of an ensemble of interfacial molecules can be inhomogeneously broadened. The asymmetric out-of-plane potential may result in differing static and dynamic solvation of the adsorbate. The solvation then becomes a function of the out-of-plane angle  $\theta$ . That is, it is possible that those C314 at the air/water interface with large angle  $\theta$  (lying nearly flat) could be more strongly solvated and therefore red-shifted in comparison to those with a smaller angle  $\theta$  (standing up). The dynamics of water solvation could be different as well, due to differing water environments, i.e., different H<sub>2</sub>O/adsorbate and H<sub>2</sub>O/H<sub>2</sub>O interactions.

At room temperature, bulk solutes rapidly sample the manifold configurations of the solvent environment. This yields homogeneous broadening of the molecule's electronic spectra. Interfacial adsorbates, however, rotate more slowly than in the bulk liquid, requiring hundreds of picoseconds to sample all of the different surface configurations. This implies that the spectrum of an ensemble of molecules at a liquid interface could be inhomogeneously broadened on the solvation time scale and that individual molecules would spectrally diffuse by rotation throughout the entire inhomogeneous line.

Static measurements of SH spectra at interfaces may be, but are not necessarily, sensitive to the differing solvation environments at the interface. The SH signal depends on the orientational average of the microscopic hyperpolarizabilities of adsorbates at the interface. The number of nonzero hyperpolarizability elements contributing to the macroscopic polarization is determined by the symmetry of the molecule and its electronic

structure. Experimentally, two elements of the macroscopic polarization,  $\chi_{zz}^{(2)}$  and  $\chi_{xx}^{(2)}$ , can be isolated by the proper choice of fundamental and SH analysis polarizations. If the SH response of the adsorbate molecule can be described as uniaxial, then both elements have the same orientational average and  $\chi_{xx}^{(2)} = \chi_{zz}^{(2)}$ . It was previously found that the orientational and solvation dynamics did not depend on the chosen element,  $\chi_{xx}^{(2)}$  and  $\chi_{zz}^{(2)}$ , for C314 at the air/water interface. This suggests that the orientational distributions probed by  $\chi_{xx}^{(2)}$  and  $\chi_{zz}^{(2)}$  do not differ and that spectral and dynamic information obtained is for the same ensemble average of adsorbates.

Because the polarization of the pump may be varied to photoexcite well-defined orientational distributions of adsorbate, time-resolved second-harmonic experiments can be used to detect differences in the solvation dynamics that can be indicative of orientationally dependent solvation environments.

TRSHG is a form of pump–probe spectroscopy where surface solute molecules are first excited by an optical pump pulse and then monitored by detecting the second harmonic generated by a time-delayed optical probe. While the pump may excite solute beyond the surface, the technique only monitors the interfacial solute molecules due to the surface specificity of SHG. The SHG signal is strongly dependent on being two-photon resonant with either the ground-state or the excited-state solute molecules. The strategy to detect orientationally dependent electronic excited-state solvation is to excite the  $S_0 \rightarrow S_1$  transition of the C314 molecules with light polarized in the plane of incidence (P-polarized pump) or light polarized perpendicular to the plane of incidence (S-polarized pump) and then monitor the change in SH probe signal as the  $S_1 \rightarrow S_0$  transition energy changes with solvation. Pumping with a P-polarized pump will excite molecules with transitions predominately out-of-plane (standing up). Pumping with an S-polarized pump will preferentially excite molecules with transitions in-the-plane (lying flat).

Differences in the amplitude and decay kinetics with different pump polarizations indicate that the solvation environment for out-of-plane-oriented and in-the-plane-oriented adsorbates is not the same. Although the dynamics show a different solvent environment for “in” vs “out” of plane adsorbates, the static spectrum would not show this difference, because the spectrum at the interface and bulk solution is broad relative to the small difference between the “in” vs “out” of plane spectral peaks. Since the TRSHG decay kinetics depends on both the spectral position, line shape of the solute, and the motion of the solvent, the decay kinetics may be analyzed to indicate whether the observed solvation dynamics depends on either or both static effects or on solvent motions that depend on the orientation of the adsorbate at the interface. It is possible that the motion of the water for a certain orientation of solute could differ and/or the spectrum of the solute is dependent on the orientation of the solute. This latter possibility could lead to different kinetics, since the kinetics depend on the wavelength of the probe and the evolution of the spectral envelope with time.

In the present study, time-resolved second-harmonic solvation dynamics experiments were performed on coumarin 314 at the air/water interface for S and P polarizations of a 420 nm pump at probe wavelengths of 840 nm (SH at 420 nm) and 900 nm (SH at 450 nm). It will be shown that the results indicate that the observed difference in the S- vs P-pumped solvation dynamics probed at 840 nm has its origin in the difference of the static solvation of in-plane vs out-of-plane molecules. This indicates that C314 is inhomogeneously broadened at the air/water interface by its orientational distribution. This report presents the first evidence of inhomogeneous broadening of a

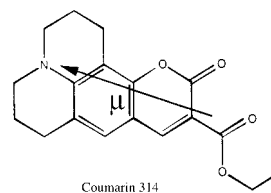


**Figure 1.** Coumarin 314. The arrow shows the direction of the permanent dipole moment and the transition dipole moment of the  $S_0$  to  $S_1$  transition.

solute by the asymmetric environment at a liquid interface. We thus see that the solvation dynamics for “in” vs “out” of plane oriented molecules is a much more sensitive probe of interface inhomogeneous broadening than static spectral measurements.

Following this introduction, section 2 will present the experimental methods. Section 3 will discuss theoretical aspects of SH spectra, and the SH spectra of C314 at the air/water interface will be presented. Section 4 will discuss the polarization dependent TRSHG results for C314 at the air/water interface. The polarization dependent kinetics will be analyzed to show that the static solvation differs for the in- and out-of-plane molecular adsorbates. Section 5 will conclude with discussion and remarks.

## 2. Experimental Section

The probe molecule chosen for this study was coumarin 314 (C314) (Figure 1). C314 was obtained commercially (Acros) and used without further purification. All solution concentrations were measured by UV/vis spectroscopy. The solution pH was 6.5. All experiments were performed at 23 °C.

C314 is a water-soluble ester that is surface active. It was found from surface tension measurements that the surface population of C314 was less than  $5 \times 10^{13}$  molecules/cm<sup>2</sup> at the bulk saturation concentration of 30  $\mu$ M. Experiments were typically run at a 26  $\mu$ M bulk concentration to maximize signal. No change in dynamics was observed with a 14  $\mu$ M bulk solution. This indicates that energy transfer and dimerizations were not factors in these experiments. C314 is ideal for SH spectroscopy using femtosecond Ti:sapphire lasers because the electronic origin provides a strong two-photon resonance enhancement to the SH from an 840 nm fundamental probe. C314 has an extinction coefficient of 45 000 L/M cm, which allows for substantial excitation with a low-power pump.

The TRSHG setup to detect electronic excited-state solvation dynamics is a pump–probe geometry similar to the one described in Figure 2 of ref 11. Briefly, a regeneratively amplified Ti:sapphire laser (Clark MXR) was used to generate pulses of about 100 fs duration, 1 mJ energy at 840 nm, and at a repetition rate of 1 kHz. The pump excitation light at 420 nm was obtained by frequency doubling the fundamental. A 500 nJ pump pulse was focused by a 1 m fl lens to a 1 mm diameter spot size at the interface and directed to the sample at an angle 70° from normal. The pump intensity was at all times well below saturation. A half-wave plate followed by a quarter-wave plate (both zero order quartz at 420 nm) was used to control the polarization. The linear polarizations were verified to be better than 300:1.

Part of the fundamental beam served as the probe beam when the probe wavelength was 840 nm. The probe was sent through a half-wave plate–polarizer attenuator and then focused onto the sample by a 1 m fl lens to a 1 mm spot diameter. The probe incidence angle was close to 70° from normal. The pump and probe beams were separated by a small angle, approximately 5°, to ensure maximum temporal resolution. The polarization

of the probe and the setting of the analyzer could be varied to select the desired tensor element of  $\chi^{(2)}$ . A colored long-wave pass glass filter was placed in the probe beam immediately before the sample to block any spurious source of SH. Care was taken choosing optics that did not temporally broaden either the pump or the probe beams. The sum-frequency cross-correlation of the probe and pump from the neat air/water interface was recorded before each solvation pump-probe experiment.

A polarizer was used to select the SH signal of the desired element of  $\chi^{(2)}$ . Finally, a colored short-wave pass glass filter was used to block any remaining fundamental, and the SH was focused into a 1/4 m monochromator (Jarrell Ash) and detected by a photomultiplier tube (R4220P, Hamamatsu). The signal from the PMT was averaged by a box car gated integrator (SRS) with a typical effective time constant of 300 ms. Laser stability was excellent (<1% shot to shot), so shot to shot normalization was not necessary. The box car signal was digitized by a computer A/D board (National Instruments) and the SH was recorded as a function of pump-delay by the computer (Apple Macintosh). Typically 40 data sets were averaged at each pump polarization.

A shallow Teflon beaker was used to contain the C314 solution. This beaker was rotated at 1 rpm with the probe spot 1 cm off axis in order to minimize any heating or other photoinduced processes in the pump/probe region of the surface. No sample degradation was observed. The measured kinetics did not change upon reduction of power by 50%.

### 3. Second-Harmonic Spectra: Static Solvation and Polarity at the Air/Water Interface

The intensity of the second harmonic generated at an interface as a function of fundamental frequency  $\omega$  is

$$I(2\omega) \propto |\chi_{\text{water}}^{(2)} + \chi_{\text{C314,non-res}}^{(2)} + \chi_{\text{C314,res}}^{(2)}(\omega)|^2 \quad (1)$$

The terms  $\chi_{\text{water}}^{(2)}$  and  $\chi_{\text{C314,non-res}}^{(2)}$  represent contributions from states far off resonance and therefore have a weak dependence on frequency  $\omega$ . The term  $\chi_{\text{C314,res}}^{(2)}(\omega)$  represents the contribution of the ground to first excited-state transition of C314, which is two-photon resonant with the fundamental laser frequency. The measured SH intensity at  $2\omega$  for the air/water interface is normalized to the reflected SH intensity from a thin plate of quartz at the same frequency to eliminate any dependence on laser intensity or pulse duration. Within the wavelength region probed (790–880 nm) the second-order susceptibility of quartz is constant. The frequency dependence of  $\chi_{\text{C314,res}}^{(2)}(\omega)$  can be expressed using perturbation theory and a simple model of dephasing as described in refs 12–14; see also section 4 below. The normalized SH spectra can then be fit to a form of eq 1 where the frequency dependence is made explicit

$$I_{2\omega} \sim |A' + \frac{u}{(\omega_m - 2\omega + i\Gamma)}|^2$$

Thus,

$$I_{\text{norm}}(2\omega) \propto |A + \frac{u\Delta}{\Delta^2 + \Gamma^2} + i\frac{u\Gamma}{\Delta^2 + \Gamma^2}|^2 \quad (2)$$

where

$$\Delta = \omega_{\text{max}} - 2\omega = \frac{1}{\lambda_{\text{max}}} - \frac{1}{\lambda_{2\omega}}$$

and  $A$  is the nonresonant magnitude,  $u$  is the resonant magnitude,

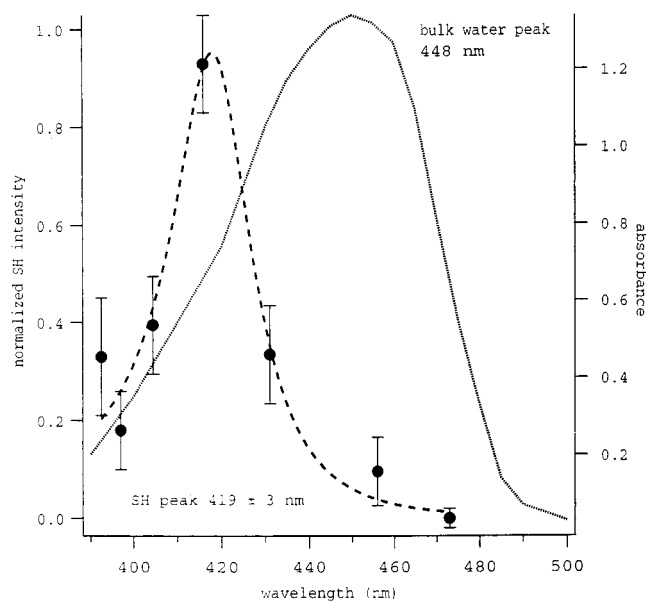


**Figure 2.** Surface second-harmonic spectra of coumarin 314 at the air/water interface. The solid circles are the normalized SH intensity vs SH wavelength. The dashed line is the SH spectral fit, described in the text, which gives a spectral peak at  $419 \pm 3$  nm. The dotted line is the bulk water absorbance spectra of coumarin 314 in a 1 cm fused silica cell. The absorbance peak is 448 nm. The bulk concentration of coumarin 314 was  $30 \mu\text{M}$  for both spectra.

$\Gamma$  is the line width, and  $\lambda_{\text{max}}$  is the transition wavelength.  $A$ ,  $u$ ,  $\Gamma$ , and  $\lambda_{\text{max}}$  are parameters which can be obtained by fitting eq 2 to the second-harmonic spectra.

The surface second-harmonic spectra of coumarin 314 at the air/water interface is shown in Figure 2. The solid circles are the normalized SH intensity for the  $\chi_{\text{C314,res}}^{(2)}$  element vs SH wavelength. The dashed line is the SH spectral fit to eq 2, described in the text, giving a spectral peak  $\lambda_{\text{max}} = 419 \pm 3$  nm and a line width  $\Gamma = 18 \pm 3$  nm. For comparison, the dotted line is the bulk water absorbance spectra of coumarin 314 in a 1 cm fused silica cell. The bulk water absorbance peak is 448 nm and the width is 28 nm. The bulk concentration of coumarin 314 was  $30 \mu\text{M}$  for both spectra.

The spectral maximum of the fit is about 3 nm to the red of the intensity maximum of the SH itself, due to the interference between the resonant and nonresonant terms in eq 1. This effect in the SH spectra has been previously noted.<sup>12,13</sup> It has been shown that the homogeneous line width broadening of the second-order process is not the same as that of the linear case and that the second-order process should yield a narrower line width than the linear case, which is consistent with the data. The measured transition wavelength of  $\lambda_{\text{max}} = 419 \pm 3$  nm is in good agreement with  $\lambda_{\text{predicted}} = 417$  nm, buttressing the conclusion of earlier studies that the interfacial polarity can be obtained from the bulk polarities of the bulk media that border the interface. In the following section, results are reported of the dynamic solvation of excited-state C314 at the air/water interface. It will be shown that the SH kinetics are dependent on both static and dynamic solvation and that by changing the polarization of the pump light, small differences in the static solvation depending on orientation can be observed.

## 4. Orientationally Dependent Excited State Solvation Dynamics of Coumarin 314 at the Air/Water Interface

**4.1. Introduction to Second-Harmonic Detection of Interfacial Solvation Dynamics.** Traditional fluorescence experi-

ments in bulk liquids have related the time evolution of the solvent to the Stokes shift response function

$$C(t) = \frac{\omega(t) - \omega(\infty)}{\omega(0) - \omega(\infty)} \quad (3)$$

where  $\omega(0)$ ,  $\omega(\infty)$ , and  $\omega(t)$  are the optical frequencies that correspond to the fluorescence emission maxima of the solute molecule immediately after the photon is adsorbed, at the time when the solute and solvent have reached equilibrium, and at intermediate times  $t$  as the solute transition energy changes as the solvent reorganizes.

There have been several measurements of the solvation dynamics in bulk water using conventional time-resolved fluorescence. In general, the decay of  $C(t)$  was found to be biexponential. Measurements using 7-dimethylaminocoumarin-4-acetate yielded time constants of  $\tau_1 = 160$  fs and  $\tau_2 = 1.2$  ps, with an amplitude-weighted average solvation time of  $\langle\tau_s\rangle = 860$  fs.<sup>15</sup> Measurements using coumarin 343 yielded time constants of  $\tau_1 = 250$  fs and  $\tau_2 = 960$  fs, with an amplitude weighted average solvation time of  $\langle\tau_s\rangle = 610$  fs.<sup>16</sup> More recent measurements on C343 with better time resolution show an additional sub-100 fs component.<sup>17</sup> C343 is structurally very similar to C314 (which is the solute used in this work). The ethyl ester group in C314 is replaced with a carboxylic acid group in C343.

In the preliminary study reported in ref 7, we reported a single measurement of the electronic excited-state solvation dynamics of coumarin 314 (C314) at the air/water interface. The interfacial C314 was pumped 70° from normal incidence with the pump light S-polarized at 420 nm. The  $\chi_{xx}^{(2)}$  susceptibility element was selected by polarizing the 840 nm probe 45° with respect to the normal and detecting the S-polarized component of the second harmonic (at 420 nm) as a function of delay time, yielding  $\chi_{xx}^{(2)}(t)$ . The data were fit to a single-exponential decay giving a solvation decay time of  $\tau_s = 790 \pm 30$  fs (see Figure 3 in ref 7)

Our preliminary study demonstrated that solvation can be studied by TRSHG and showed that the air/water solvation time for C314 was similar to the average values of 690–880 fs previously measured in bulk water. Unlike bulk water, only one solvation component greater than 100 fs was observed. It was proposed that only the slower component was observed due to the temporal resolution of the instrument. The subsequent results of this subsequent work for the solvation decay measured at a probe wavelength of 900 nm (SH at 450 nm) did show a faster 200 fs component. Furthermore, subsequent experiments showed a difference in decay times at 840 nm probe for S vs P pumping. This result indicates that the solvation dynamics at the interface depends on the orientation of the solute.<sup>8</sup>

There are two possible methods to relate  $C(t)$  to experimental measurements of the time dependent,  $\chi^{(2)}(t)$  obtained from SH measurements (as in ref 7). A sequence of measurements of  $\chi^{(2)}(t)$  taken at many wavelengths could be used to spectrally reconstruct the time dependent second-harmonic spectrum and extract  $\omega(0)$ ,  $\omega(\infty)$ , and  $\omega(t)$  to compute  $C(t)$  directly. Alternately, it is in principle possible to choose a probe wavelength where the measurement of  $\chi^{(2)}(t)$  is directly proportional to  $C(t)$ . This latter method, which is called the linear wavelength method,<sup>18,19</sup> relies on a linear relationship between the magnitude of the SH response at the chosen wavelength and the solvent coordinate  $q(t)$  (see Figure 2 in ref. 7). In fluorescence spectroscopy, the linear wavelength can be predicted by analyzing the fluorescence spectra for a series of solvents. The

solvent coordinate  $q(t)$  can be correlated to each equilibrium spectrum by a solvent polarity parameter (such as  $E_T(30)$ ), which is the basis for the most commonly used polarity scale.<sup>12,13</sup> It is assumed that the dynamic solvation of a liquid at time  $t$  can be treated as equivalent to the equilibrium polarity of some other solvent at  $t = \infty$ . That is, the solvation coordinate,  $q_1(t)$  of liquid 1 equals the solvation coordinate  $q_2(\infty) \approx E_T(30)$  in liquid 2. Since the fluorescence spectral peak frequency is linearly proportional to  $E_T(30)$ , it follows that a one-to-one linear correspondence can be made between the fluorescence at each time  $t$  and the equilibrium spectra of the same solute in series of solvents. This implies that the polarity series of fluorescence spectra can be analyzed to find a wavelength for which the fluorescence intensity varies linearly with polarity. Such a wavelength corresponds to the solvation experiment single wavelength, since the solvation coordinate  $q_1(t)$  is linearly related to the polarity parameter  $E_T(30)$  in the solvent series. See refs 18 and 19 for a more detailed description of this analysis.

The fluorescence linear wavelength procedure works remarkably well and yields the same solvation kinetics, within 10–15%, as the more complicated spectral reconstruction method.<sup>18,19</sup> The dynamic solvation effect itself is influenced by the polarity of the liquid. A more polar liquid will undergo a greater dynamic solvation for the same change in solute dipole moment, for example. As a practical matter, spectral reconstruction experiments show that while the fluorescence peak shifts with solvation from  $t = 0$  to  $t = \infty$ , the spectral line shape and quantum yield change a comparatively small amount. Under these conditions, a quasilinear wavelength can still be found. Viewed from this perspective, the linear wavelength corresponds to a region where the static fluorescence spectral line shape is itself quasilinear over the region from the measurement wavelength to that wavelength minus the Stokes shift. This simple analysis to determine the linear wavelength shows that there is often a window of quasilinear wavelengths where the solvation kinetics will differ marginally from spectral reconstruction kinetics.<sup>18,19</sup>

The method for predicting the linear wavelength for a second-harmonic pump–probe electronic excited-state solvation dynamics measurement is as follows. The energy of the excited state is obtained from fluorescence measurements of coumarin 314 in a series of solvents of different polarity. The transition energy at the interface is obtained using our observation that the transition energy at the interface is equal to one-half of the transition energies in the two bulk media that form the interface. We then calculate the position of the SH peak for the various interfacial transition energies. The spectral width corresponds to the measured SH width at the probe wavelength. We include the interference effects with the ground-state molecules to calculate where the peak would occur in the SH measurement. The intensity of the SH at various wavelength obtained for the various interfaces are then plotted against  $E_T(30)$ . The wavelength for which the SH intensity scales linearly with the polarity parameter  $E_T(30)$  is a linear wavelength. Previously, for C314 at the air/water interface, 840 nm was identified as a reasonable SH linear wavelength from analysis of the polarity series fluorescence spectra of C314. However, a detailed consideration of ground state SH interference effects was not made. Further solvation experiments have shown that 840 nm is not linear and that 900 nm is a linear wavelength. It should be noted, though, that the nonlinearity of 840 nm can be utilized in order to identify differences in the S- and P-pumped interfacial SH spectra should their decay kinetics differ. The 840 nm data together with the 900 nm data will be used to show that the

electronic spectra of C314 at the air/water interface is inhomogeneously broadened by C314's out-of-plane angle.

**4.2. Theory of Second Harmonic Detection of Orientationally Dependent Interfacial Solvation Dynamics.** Elements of the theory of the measurement of interfacial electronic excited-state solvation dynamics by TRSHG have been presented previously in ref 7. In that work, the possibility that the electronic spectra of C314 at the air/water interface could have an orientational dependence was not considered. To interpret the results to include the possibility of orientation dependence, the theory of SH detection of solvation dynamics will be presented with special attention to orientational dependence and ground-state interference effects.

The second-harmonic signal field generated at the interface is proportional to the square root of the experimentally measured intensity,  $E(2\omega) = \sqrt{I(2\omega)}$ . The SH field is proportional to the induced second-order nonlinear polarization,  $E(2\omega) \propto P^{(2)}(2\omega)$ . The SH polarizations with components  $i, j$ , and  $k$  can be written as the product of the probe electric field acting twice and the second-order nonlinear susceptibility  $\chi_{ijk}^{(2)}$ ,

$$P_i^{(2)}(2\omega; t) = \chi_{ijk_{\text{res}}}^{(2)}(2\omega, \omega, \omega; t) E_j(\omega) E_k(\omega) + \chi_{ijk_{\text{non-res}}}^{(2)}(2\omega, \omega, \omega; t) E_j(\omega) E_k(\omega) \quad (4)$$

where the subscripts  $i, j$ , and  $k$  are determined by the polarization of the analyzed SH and the probe fundamental. Here the nonlinear susceptibility tensor has been separated into the resonant response of the solute and the nonresonant response of the solute and interfacial solvent. All spectral dynamics are included in the resonant portion of the tensor, because it is only the change in resonance as the solvent relaxes that leads to the time dependent solvation and the change in the SH signal with time. The resonant surface second-order nonlinear susceptibility tensor for a ground-state ensemble of solute chromophores at the air/water interface can be expressed as<sup>1</sup>

$$\chi_{ijk_g}^{(2)}(e\varphi) = N_g \sum \langle T_{lmn}^{ijk} \alpha_{lmn_g}^{(2)}(\omega, \theta) \rangle_g \quad (5)$$

where  $T_{lmn}^{ijk}$  is the direction cosine matrix that transforms the laboratory frame ( $i, j, k$ ) into the molecular frame ( $l, m, n$ ),  $N_g$  is the number of ground-state molecules at the surface at equilibrium,  $\alpha_{lmn_g}^{(2)}(\omega, \theta)$  is the ground-state molecular hyperpolarizability for the  $l, m, n$  axes and  $\langle \rangle_g$  denotes the orientational ensemble average. The interfacial ground-state hyperpolarizability,  $\alpha_{lmn_g}^{(2)}(\omega, \theta)$ , is given an explicit dependence on the probe frequency  $\omega$  and the out-of-plane angle  $\theta$ . It is this dependence that is responsible of the orientational inhomogeneity of the interfacial SH spectra.

In general, an interfacial solute is distributed with out-of-plane angle  $\theta$  and in-plane angle  $\varphi$ . The transition dipole moment of the solute taken to be the reference axis of the molecule (see Figure 1 ref 11 for a schematic of this coordinate system for C314 at the air/water interface). Since the interfacial forces in-the-plane are isotropic, there is no in-plane  $\varphi$  dependence to  $\alpha_{lmn_g}^{(2)}(\omega, \theta)$ . Traditional treatments of the interfacial hyperpolarizability do not assume any dependence on the out-of-plane angle  $\theta$  and neglect the possibility that the orientation of a molecule could affect its electronic transition energy.

The orientational average in eq 5 is sensitive to the orientational probability distribution of solute at the liquid interface. At  $t < 0$  (i.e., the probe arrives before the pump in a TRSHG experiment), all molecules are in their ground-state equilibrium

distribution. The probability distribution for finding a ground-state adsorbate with out-of-plane angle  $\theta$  and in-plane angle  $\varphi$  is  $\rho_g(\theta)$ . The SH resonant susceptibility before pumping is

$$\chi_{ijk_{\text{res}}}^{(2)}(t < 0) = N_g \sum \langle T_{lmn}^{ijk} \alpha_{lmn_g}^{(2)}(\omega, \theta) \rangle_{\rho_g(\theta)} \quad (6)$$

The pump pulse photoselects an anisotropic subset of molecules from the interfacial orientational distribution, thereby altering the orientational average in eq 6. By choosing the pump polarization and geometry, the photoselection will excite different subsets of  $\rho_g(\theta)$ . The pump geometry is assumed to be incident at an angle  $\vartheta$  with respect to the surface normal and its electric field is polarized at an angle  $\Theta$ . For P polarization,  $\Theta = 0^\circ$ , and for S polarization,  $\Theta = 90^\circ$ . The probability of excitation is related to the square of the pump electric field at incidence angle  $\vartheta$  and polarization  $\Theta$  projected onto the transition dipole moment of solute chromophore oriented at  $\theta$  and  $\varphi$ .

The distribution of molecules excited by the pump pulse at  $t \geq 0$  will be denoted  $\rho_e(\Theta; \theta, \varphi)$  where  $\Theta$  denotes the pump polarization (S or P). The number of excited molecules oriented at  $\theta$  will be proportional to  $N_e \rho_e(\Theta; \theta, \varphi)$ , with  $N_e$  being the total number of interface excited molecules at  $t = 0$ . The number of ground-state molecules remaining oriented at  $\theta$  and  $\varphi$  is proportional to  $N \rho_g(\theta, \varphi) - N_e \rho_e(\Theta; \theta, \varphi)$ , where  $N$  is the total number of molecular adsorbates. The excited and ground-state distributions do not change during the time scale of excited-state solvation so the distribution,  $\rho_e(\Theta; \theta, \varphi)$ , and  $N_e$  can be treated as static. On a longer time scale,  $\rho_e(\Theta; \theta, \varphi)$  evolves due to interfacial orientational dynamics and ground state recovery, which has been investigated experimentally and theoretically in ref 11. The time dependent change in SH for solvation dynamics experiment is due to a time dependent change in the resonant denominator of the excited-state hyperpolarizability  $\alpha_{lmn_e}^{(2)}(\omega, \theta; t)$ , because it is only the excited molecules that experience solvent reorganization following photoexcitation and not the ground-state molecules.

If at time  $t = 0$  the adsorbant is pumped by a one-photon resonant polarized pump pulse, the probe SH resonant susceptibility at time  $t$  is given by

$$\chi_{ijk_{\text{res}}}^{(2)}(\theta; t) = (N - N_e) \sum \langle T_{lmn}^{ijk} \alpha_{lmn_g}^{(2)}(\omega, \theta) \rangle_{\rho_g(\theta)} + N_e \sum \langle T_{lmn}^{ijk} \alpha_{lmn_e}^{(2)}(\omega, \theta; t) \rangle_{\rho_e(\Theta, \theta, \varphi)} \quad (7)$$

It is the right-hand term in eq 7 that contains all of the excited-state dynamics and the sensitivity to the pump polarization  $\Theta$ . It should be noted that the susceptibilities are complex quantities and the expression for the polarization must include the resonant background (left-hand side of eq 4) and the nonresonant susceptibility contained in eq 4. The number of nonzero hyperpolarizability elements  $\alpha_{lmn}^{(2)}$  contributing to eqs 5–7 is determined by the symmetry of the molecule and its electronic structure. Since the only strong SH resonance enhancement for C314 is the two-photon resonance between the ground  $S_0$  and lowest excited-state  $S_1$ , we make the approximation that C314 is a two-level system. Furthermore, we make the approximation that the C314 has uniaxial symmetry, which we found to be experimentally supported by the observation that the dynamics measured by  $\chi_{xz}^{(2)}$  and  $\chi_{zx}^{(2)}$  are the same for C314 at the air/water interface.<sup>8</sup> In this case there is only one nonzero hyperpolarizability element for the ground state,  $\alpha_{\zeta\zeta\zeta_g}^{(2)}$ , and the excited state,  $\alpha_{\zeta\zeta\zeta_e}^{(2)}(\omega, \theta; t)$ .

The direction cosine matrix element transforming the single uniaxial hyperpolarizability  $\alpha_{\zeta\zeta\zeta_g}^{(2)}$  into the lab frame is  $\sin^2 \theta$

$\cos \theta \cos^2 \varphi$  for both  $\chi_{xx}(^{(2)})$  and  $\chi_{zz}(^{(2)})$ . The sensitivity of SH to the out-of-plane orientation is given by the terms  $\sin^2 \theta \cos \theta$ . For coumarin 314, eq 7 can be expressed as

$$\chi_{xx}(^{(2)})(\theta;t) = (N - N_e) \langle \sin^2 \theta \cos \theta \cos^2 \varphi \alpha_{\zeta\zeta\zeta\zeta}^{(2)}(\omega, \theta) \rangle_{\rho_g(\theta)} + N_e \langle \sin^2 \theta \cos \theta \cos^2 \varphi \alpha_{\zeta\zeta\zeta\zeta}^{(2)}(\omega, \theta) \rangle_{\rho_e(\Theta, \theta, \varphi)} \quad (8)$$

The second-harmonic spectral line shape can be expressed by perturbation theory assuming a simple phenomenological pure dephasing function as in refs 12–14. Since for this experiment the SH from C314 is only two-photon resonant, the expression for the resonant part of the ground-state hyperpolarizability  $\alpha_{\zeta\zeta\zeta\zeta}^{(2)}(\omega, \theta)$  can be simplified and given as a function of the fundamental laser frequency  $\omega$  and the second harmonic  $2\omega$  by

$$\alpha_{\zeta\zeta\zeta\zeta}^{(2)}(\omega, \theta) \propto \frac{\mu_{ge}\sigma_g}{(\omega_{ge}(\theta) - 2\omega + i\Gamma_{ge})} + B \quad (9)$$

where  $\mu_{ge}$  is the transition dipole matrix element between the ground and excited state,  $\omega_{ge}(\theta)$  is the transition frequency between the ground and excited state for a molecule with orientation  $\theta$ ,  $\Gamma_{ge}$  is the line width for the transition, and  $\sigma_g$  contains other constant terms. For C314, the only resonant quantity in the denominator is the second-harmonic transition at  $2\omega$  between  $S_0$  and  $S_1$ . For the sake of brevity, the nonresonant terms for C314 in eq 9 have been gathered in the constant  $B$ . The frequency  $2\omega$  is determined by the probe laser and is not varied. Since solvent reorganization occurs only for the excited states and not the ground state, the transition energy  $\omega_{ge}(\theta)$  for the ground state does not change and thus the hyperpolarizability  $\alpha_{\zeta\zeta\zeta\zeta}^{(2)}(\omega, \theta; t)$  is constant in time.

The excited-state hyperpolarizability  $\alpha_{\zeta\zeta\zeta\zeta}^{(2)}(\omega, \theta; t)$ , however, is *not* constant in time, because the  $S_1 \rightarrow S_0$  transition energy for the excited molecules  $\omega_{eg}(\theta; q(t))$  depends on the solvation coordinate  $q(t)$ . As the water reorganizes around the excited-state dipole of C314, the transition frequency  $\omega_{eg}(\theta; q(t))$  changes in time. The time dependent hyperpolarizability  $\alpha_{\zeta\zeta\zeta\zeta}^{(2)}(\omega, \theta; t)$  is given analogous to eq 9

$$\alpha_{\zeta\zeta\zeta\zeta}^{(2)}(\omega, \theta; t) \propto \frac{\mu_{ge}\sigma_e}{(\omega_{eg}(\theta; q(t)) - 2\omega + i\Gamma_{eg})} + B \quad (10)$$

where  $B$  contains the nonresonant terms. Note that initially at  $t = 0$ , before any solvation takes place, the microscopic hyperpolarizabilities are equal in magnitude but opposite in sign,  $\alpha_e^{(2)} = -\alpha_g^{(2)}$  for the two-state model.

The time-resolved second-harmonic signal for excited-state solvation is given by evaluation using eqs 4 and 8. Note that eqs 4 and 8–10 are complex, and it is necessary to evaluate eq 4 while the complex form of each susceptibility is maintained. The solvation time dependence in the resonant SH susceptibility in eq 8 is a consequence of the time dependence of the solvation on the value of  $\omega_{eg}(\theta; q(t))$  in eq 10, whereas the pump polarization dependence is a consequence of  $\rho_e(\Theta, \theta, \varphi)$ , which selects the orientational average in eq 8. The precise form of the time dependence depends on the choice of the fundamental probe frequency  $\omega$  in eq 10.

**4.3. Results and Discussion of Orientationally Dependent Excited-State Solvation Dynamics of Coumarin 314 at the Air/Water Interface.** *4.3.1. Second-Harmonic Response to Solvation Dynamics for 840 nm Probe.* The orientationally dependent second-harmonic response to the electronic excited-state solvation of 30  $\mu\text{M}$  coumarin 314 at the air/water interface

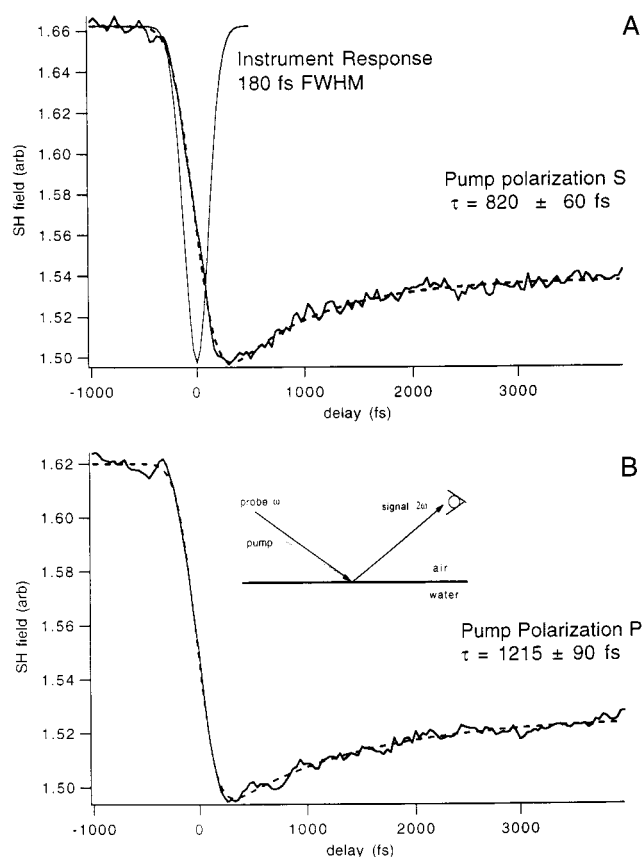


**Figure 3.** Orientational dependent dynamics of electronic excited-state solvation of coumarin 314 at the air/water interface for the 840 nm probe (SH at 420),  $\chi_{xx}(^{(2)})$  element. The pump was at 420 nm. (A) Pump polarization S (in-plane). The SH field is plotted vs pump delay. The dashed line is a fit to a single-exponential giving a decay time of  $820 \pm 60$  fs. The sum frequency cross correlation of the pump and the probe with  $\text{fwhm} = 180$  fs is shown in the inset to illustrate the temporal resolution. (B) Pump polarization P (out-of-plane). The SH field is plotted vs pump delay. The dashed line is a fit to a single-exponential, giving a decay time of  $1215 \pm 90$  fs. The inset shows the experimental geometry.

for the 840 nm probe (SH at 420) and  $\chi_{xx}(^{(2)})$  element is shown in Figure 3. The pump was at 420 nm, directly resonant with the electronic transition of C314 at the air/water interface. The pump and probe beams are both  $70^\circ$  from normal incidence, separated  $5^\circ$  in the plane. The solvation decay and fit for the S-polarized pump (in-plane) is shown in Figure 3A. The SH field is plotted vs pump-probe delay. The dashed line is a fit to a single-exponential, giving a decay time of  $\tau_S(420 \text{ nm}) = 820 \pm 60$  fs. The baseline represents the remaining contribution of the ground states to the SH. The finding that the change in the SH signal does not recover to half of its maximum value indicates that the fully solvated excited state remains close to a two-photon resonance with the probe. The data did not yield a better fit with a biexponential decay function than the single-exponential fit. The sum frequency cross correlation of the pump and the probe with  $\text{fwhm} = 180$  fs is shown in the inset to illustrate the temporal resolution.

The time-resolved SH solvation dynamics for P-polarized pump (out-of-plane) is shown in Figure 3B. The SH field is plotted vs pump delay. The dashed line is a fit to a single-exponential, giving a decay time of  $\tau_P(420 \text{ nm}) = 1215 \pm 90$  fs. The inset shows the experimental geometry. The result that  $\tau_S(420 \text{ nm}) \neq \tau_P(420 \text{ nm})$  implies either that the dynamics of the solvent motions are different for absorbates that are preferentially oriented more parallel to the interface (S pumping)

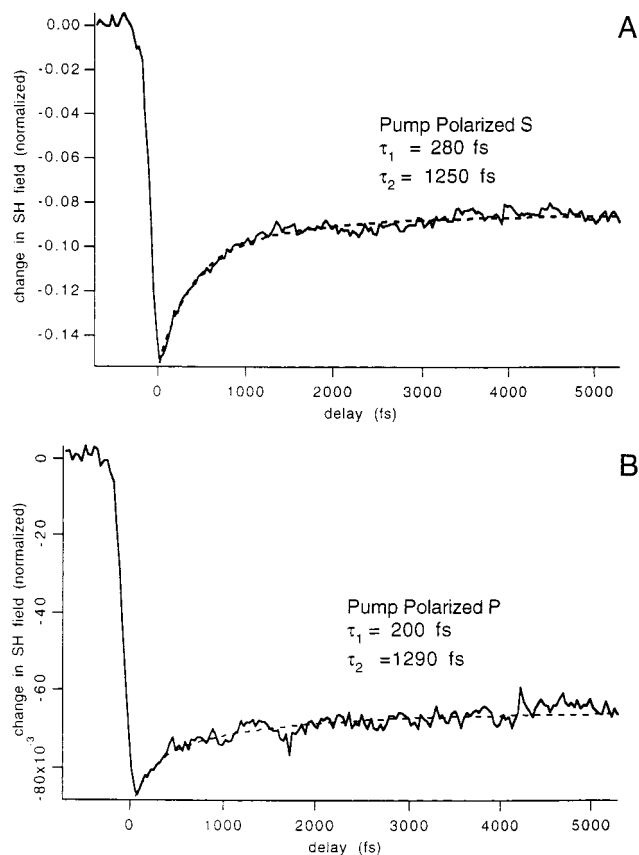


**Figure 4.** Electronic excited-state solvation dynamics of coumarin 314 at the air/water interface for 900 nm probe (SH at 450),  $\chi_{xx}^{(2)}$  element. The pump was at 420 nm. The data are best fit to a sum of two exponential decays. (A) Pump polarization S (in-plane). The normalized change in SH field is plotted vs pump delay. The dashed line is a fit to a biexponential giving decay time constants of  $\tau_1 = 280 \pm 50$  fs and  $\tau_2 = 1250 \pm 80$  fs. (B) Pump polarization P (out-of-plane). The normalized change in SH field is plotted vs pump delay. The dashed line is a fit to a biexponential giving decay time constants of  $\tau_1 = 200 \pm 50$  fs and  $\tau_2 = 1290 \pm 80$  fs.

compared with those preferentially oriented more perpendicular to the interface (P pumping) or that the static excited-state spectra differ for the S- and P-pumped cases. This latter static effect on the solvation dynamics results from the dependence of the observed solvation time dependence on the probe frequency. This has been observed in bulk solvation studies, where it was seen that fluorescence intensity can increase or decrease with time, depending on the fluorescence wavelength that is monitored. The time constants for the  $\chi_{xx}^{(2)}$  element (not shown) were the same as  $\chi_{xx}^{(2)}$  for both S and P pumping within the signal-to-noise ratio. The difference in S- and P-pumped dynamics shows that the adsorbed coumarin 314 molecules have a distribution of orientational environments. If the coumarin orientation was narrow, i.e., essentially a single  $\theta$ , then the kinetics would have to be the same for S- and P-pumped experiments.

**4.3.2. Second-Harmonic Response to Solvation Dynamics for 900 nm Probe.** The second harmonic response to the electronic excited-state solvation for 30  $\mu$ M coumarin 314 at the air/water interface for the 900 nm probe (SH at 450) and the  $\chi_{xx}^{(2)}$  element is shown in Figure 4. The pump was at 420 nm and the geometry is identical to the 840 nm probe experiment in section 4.3.1. The data are best fit to a sum of two exponential decays. The solvation decay and the fit for the S-polarized pump (in-plane) is shown in Figure 4A. The normalized change in the SH field is plotted vs pump delay. The dashed line is a fit to a

biexponential giving decay time constants of  $\tau_{S1}(450 \text{ nm}) = 280 \pm 50$  fs and  $\tau_{S2}(450 \text{ nm}) = 1250 \pm 80$  fs. The solvation decay and fit for the P-polarized pump (out-of-plane) is shown in Figure 4B. The normalized change in SH field is plotted vs pump delay. The dashed line is a fit to a biexponential, giving decay time constants of  $\tau_{P1}(450 \text{ nm}) = 200 \pm 50$  fs and  $\tau_{P2}(450 \text{ nm}) = 1290 \pm 80$  fs. The time constants for the  $\chi_{xx}^{(2)}$  element (not shown) were the same for both S and P pumping and the same as the  $\chi_{xx}^{(2)}$  measurements.

Unlike the result for the 840 nm probe, the solvation time constants at 900 nm were the same for the S- and P-pumped experiments within our experimental precision. This implies that the dynamics of solvent motions is identical for both the S and P polarization selected distributions. If the solvent motions depended on the orientation of the excited adsorbates, then the observed solvation time dependence or S pumping should be different, regardless of probe wavelength, i.e., 840 nm vs 900 nm probe. We thus conclude that the difference at 840 nm in the dynamics for S vs P pumping is due to a spectral shift that depends on the orientation of the adsorbate excited.

**4.3.3. Analysis of 840 and 900 nm Probe Solvation Dynamics.** The differing results for the orientationally dependent second-harmonic response to the electronic excited-state solvation for 840 nm probing (section 4.3.1) and for 900 nm probing (sections 4.3.2) must be interpreted within a single consistent framework. It should be noted that regardless of the probe wavelength the orientational distribution is the same because it is determined by the pump light at 420 nm. Thus for S pumping the excited-state orientations are the same for the 840 and 900 nm probes. The same holds for P pumping. The actual water solvation motions about the excited adsorbates (not the second harmonic response) should be independent of probe wavelength, given the proper analysis. The interpretation most strongly suggested by the data is that the electronic transition energy for S- and P-excited orientational distributions of C314 at the air/water interfaces are slightly offset, due to the different intermolecular interactions of an adsorbate in a flat orientation vs a more perpendicular orientation with the interfacial and bulk solvent molecules. At 900 nm, which is a linear wavelength, we find that the solvation dynamics are identical for both the S and P distributions. The data indicate that the air/water solvation dynamics proceed with two time constants,  $\tau_1 = 200$  fs and  $\tau_2 = 1.2$  ps. This interpretation can resolve the differing time constants for S and P pumping for the 840 nm probe.

The consequences of the offset in electronic transition energy for S- and P-excited orientational distributions of C314 at the air/water interface to the second harmonic response to solvation is illustrated in Figure 5. The spectral peak of the *average* ground-state C314 ensemble at the air/water interface was found to be 419 nm in section 3. The excited-state transition, at  $t = 0$ , expected to be the mirror image, peaked as well at 419 nm. Previous experiments suggest<sup>11</sup> that the orientational distribution is peaked at an out-of-plane angle  $\theta = 80^\circ$ , implying that the static SH spectra is strongly associated with the S-polarized pump distribution of C314. A P-polarized pump would excite the smaller fraction of C314 that happened to be at a smaller angle  $\theta$  (standing more nearly normal to the surface).

As shown in Figure 5, it is proposed that the ensemble excited by P-polarized light has a spectra corresponding to the dotted curve on the left, whereas the ensemble excited by S-polarized light has a spectra corresponding to the dashed curve on the right (peak 419 nm). If the S and P peaks are offset by 5 nm, qualitative agreement with the data is obtained. The offset cannot be zero if an orientational dependent static polarity is responsible

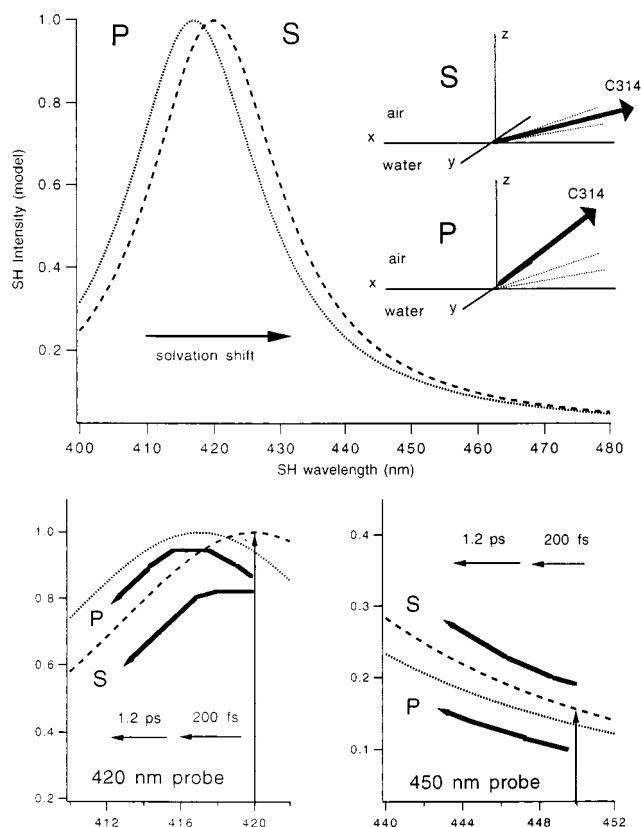


**Figure 5.** Model subcomponents of the excited-state SH spectra of coumarin 314 at the air/water interface. It is proposed that the ensemble excited by P-polarized light has a spectra corresponding to the dotted curve on the left, whereas as the ensemble excited by S-polarized light has a spectra corresponding to the dashed curve on the right. In both cases the excitation wavelength is 420 nm. The insets show the predominate out-of-plane orientation of C314 excited by S- and P-polarized light. The difference in out-of-plane angle (angle between the  $z$ -axis and the  $x$ - $y$  plane) is exaggerated for clarity. The spectral peaks of both the P and S distributions red shift with solvation, as indicated by the arrow.

for the differing S- and P-pumped solvation dynamics observed at 840 nm. The spectral peaks of both the P and S distributions red shift with solvation  $\sim 10$  nm. Bulk results indicate that about half the spectral shift occurs during the 200 fs component and the other half during the 1.2 ps component.

## 5. Discussion

The measured air/water interfacial solvation times of  $\tau_1 = \sim 200$  fs and  $\tau_2 = 1.2$  ps are in substantial agreement with measurements in bulk water by other workers. Measurements using 7-dimethylaminocoumarin-4-acetate in bulk water yielded time constants of  $\tau_1 = 160$  fs and  $\tau_2 = 1.2$  ps.<sup>15</sup> Measurements using coumarin 343 yielded time constants of  $\tau_1 = 250$  fs and  $\tau_2 = 960$  fs.<sup>16</sup> More recent measurements on C343 with better time resolution show an additional sub-100 fs component. Our apparatus does not have resolution to observe this component.<sup>17</sup> Since the dynamics are due to the water motions and water/water interactions, the water solvation times should not depend on the probe molecule. This implies that both the solute/water and water/water interactions responsible for the dynamic solvation are the same at the air/water interface as they are in bulk water.

The average measured solvation time of  $\langle \tau_S \rangle = 800$  fs is in reasonable agreement with the simple dielectric continuum model (DCM), which predicts the bulk solvation time to be equal

to the one component longitudinal dielectric relaxation time of bulk water,  $\tau_1 = 590$  fs.<sup>17,20</sup> One possibility for the agreement with the bulk prediction is that the solvation depends on long-range as well as short-range interactions of the solute with the solvent, an interpretation that is also supported by the static measurements of interface polarity.<sup>12,13</sup> Here we consider short-range interactions to mean interactions with the first solvent shell, whereas long-range interactions are from the second shell to infinity. The precise number of shells that contribute significantly to the long-range interactions is not known. The equivalence of the bulk water and air/water solvation times is also supported by molecular dynamics studies, which indicate that the bulk and surface dynamic response is nearly identical, because the solvent shell of the surface solute is nearly identical to the bulk solute.<sup>20,21</sup>

Note that while the presence of air on one side of C314 changes the polarity of the interface and the static Stokes shift, air itself does not solvate in response to the increased dipole moment of C314. Hence in this case, the dynamics are due solely to water solvation. The air/water interface is not necessarily the most general result; a liquid/liquid interface having two polarizable liquids adjacent to it would be expected to have dynamics dependent on the response of both liquids.

Previous studies have proposed that a generalized interfacial polarity scale can be developed where the polarity of the interface is the arithmetic average of the polarities of the bulk constituent phases (see eq 5 in ref 12). These polarity results indicated that the solvation interactions of the interface molecules, which determine the static electronic energy difference between the ground and excited states, are essentially the same for solute located in the bulk and in the interfacial regions. This was surprising because the local interfacial interactions with neighboring interfacial solvent molecules could be expected to differ from the solute/solvent interactions in the bulk solvent due to the asymmetry in forces present in the interfacial region. The current work finds that orientation does have an effect, but it is substantially smaller than the long-range interactions which dominate the difference in excited and ground-state solvation energies. Most of the C314 at the air/water interface is restricted to a range of out-of-plane angles near  $\theta = 80^\circ$ . This distribution, which is the one pumped by S-polarized light, has precisely the transition energy predicted by the interfacial polarity scale. A relatively smaller portion of the interfacial C314 is pumped by P-polarized light, and the difference in the interfacial energy indicated may represent the extreme effect of those C314 which happen to be more nearly normal to the interface. Thus the inhomogeneity due to orientation is both small in comparison to the interfacial line width (5 nm vs 18 nm) and small due to only a small population at wavelengths other than the wavelength predicted for the homogeneous spectra by the generalized interfacial polarity scale.

## 6. Conclusion

The electronic excited-state solvation dynamics of C314 adsorbed at the air/water interface was investigated by femto-second TRSHG. The second-harmonic spectra of C314 at the air/water interface was determined using a tunable optical parametric generator; giving a spectral peak at  $419 \pm 3$  nm. The solvatochromic shift is in good agreement with the recently proposed generalized interfacial polarity scale, which predicts that the empirical polarity parameter of the interface is the arithmetic mean of the two bulk phases. The time-resolved second-harmonic response to excited-state solvation was measured at two fundamental wavelengths (840 and 900 nm) and

with two pump polarizations (S and P). The results indicate that the static spectral peaks of the S- and P-pumped distributions are offset while the dynamic interfacial solvation proceeds with two time constants,  $\tau_1 = \sim 200$  fs and  $\tau_2 = 1.2$  ps, which are independent of C314 interfacial orientation. The slight blue shift of the C314 molecules closer to normal incidence indicates that the electronic spectra of species at the air/water interface is inhomogeneously broadened by orientation, an effect which had not been observed previously. The dynamic solvation times are close to bulk experimental values and theoretical studies which find that the air/water solvation times are close to the bulk values.

**Acknowledgment.** The authors wish to acknowledge the support of the National Science Foundation. The authors would also like to acknowledge Dr. Xiaolin Zhao and Dr. Joshua Salafsky for their technical assistance.

### References and Notes

- (1) Heinz, T. F. *Nonlinear Surface Electromagnetic Phenomena*, Eds. Ponath, H. and Stegeman, G. Elsevier: Amsterdam, 1991.
- (2) Eisenthal, K. B. *Accounts Chem. Res.* **1999**, *26*, 636.
- (3) Corn, R. M.; Higgins, D. A. *Chem. Rev.* **1994**, *94*, 107.
- (4) Brevet, P. F.; Girault, H. H. *Second Harmonic Generation at Liquid/Liquid Interfaces*, CRC Press: Boca Raton, 1996.
- (5) Hicks, J. M.; Kemnitz, K.; Eisenthal, K. B.; Heinz, T. F. *J. Phys. Chem.* **1986**, *90*, 560.
- (6) Rasing, T.; Shen, R. Y.; Kim, M. W.; Valint, J. P.; Bock, J. *Phys. Rev. A* **1985**, *31*, 537.
- (7) Zimdars, D.; Dadap, J. I.; Eisenthal, K. B.; Heinz, T. F. *Chem. Phys. Lett.* **1999**, *301*, 112.
- (8) Zimdars, D.; Eisenthal, K. B. *J. Phys. Chem. A* **1999**, *10*, 10567.
- (9) Moylan, C. R. *J. Phys. Chem.* **1994**, *98*, 13513.
- (10) Maroncelli, M.; Fleming, G. R. *J. Chem. Phys.* **1987**, *86*, 6221.
- (11) Zimdars, D.; Dadap, J. I.; Heinz, T. F.; Eisenthal, K. B. *J. Phys. Chem. B* **1999**, *103*, 3425.
- (12) Wang, H.; Borguet, E.; Eisenthal, K. B. *J. Phys. Chem. B* **1998**, *102*, 4927.
- (13) Wang, H.; Borguet, E.; Eisenthal, K. B. *J. Phys. Chem. A* **1997**, *101*, 13.
- (14) Shen, Y. R. *Annu. Rev. Phys. Chem.* **1989**, *40*, 327.
- (15) Jarzeba, W.; Walker, G. C.; Johnson, A. E.; Kahlow, M. A.; Barbara, P. F. *J. Chem. Phys.* **1998**, *92*, 7039.
- (16) Walker, G. C.; Jarzeba, W.; Kang, T. J.; Johnson, A. E.; Barbara, P. F. *J. Opt. Soc. Am. B* **1990**, *7*, 1521.
- (17) Jimenez, R.; Fleming, G. R.; Kumar, P. V.; Maroncelli, M. *Nature* **1994**, *369*, 471.
- (18) Kahlow, M. A.; Kang, T. J.; Barbara, P. F. *J. Chem. Phys.* **1988**, *88*, 2372.
- (19) Gardecki, J. A.; Maroncelli, M. *J. Phys. Chem. A* **1999**, *103*, 1187.
- (20) Benjamin, I. *Chem. Rev.* **1996**, *96*, 1449.
- (21) Benjamin, I. *Acc. Chem. Res.* **1995**, *28*, 233.